Suppression of primary electron interferences in the ionization of N_2 by 1–5-MeV/u protons

J. L. Baran,[1] S. Das,[1] F. Járai-Szabó,[2] K. Póra,[2] L. Nagy,[2] and J. A. Tanis[1]
[1]*Department of Physics, Western Michigan University, Kalamazoo, Michigan 49008, USA*
[2]*Faculty of Physics, Babes-Bolyai University, 400084 Cluj, Romania*
(Received 25 September 2007; published 25 July 2008)

Oscillatory structures associated with electron emission in 1–5-MeV H^+ collisions with N_2 have been investigated. Ratios of experimental molecular N_2 to theoretical atomic N cross sections exhibit nearly constant frequency sinusoidal oscillations that do not vary with the electron observation angle or collision velocity. The results suggest suppression of primary Young-type interferences, in sharp contrast to observations for H_2, while secondary structures attributed to intramolecular scattering are prominent. Theoretical calculations predict suppression of the primary interferences but not to the extent observed in the measurements.

DOI: 10.1103/PhysRevA.78.012710 PACS number(s): 34.50.Fa, 32.80.Fb

I. INTRODUCTION

It is well-known that electrons have both particle and wavelike properties similar to photons. A manifestation of this duality has recently been shown to occur in the ejection of electrons from H_2 impacted by fast ions [1]. Whereas electron ejection from an atom gives rise to a single outgoing ionization "wave," corresponding ejection from H_2 occurs simultaneously from both atomic centers, resulting in coherent ionization waves that can interfere. This phenomenon of interference associated with electron ejection from molecules is analogous to Young's two-slit experiment with the atomic centers acting as "slits," and was considered already more than 40 years ago in the photoionization of molecules [2,3]. Prior to recognition of this Young-type interference involving simultaneous emission from two atomic centers, Kronig [4] attributed oscillatory structures in the *K*-shell ionization spectra of heteronuclear molecules to intramolecular scattering. In the latter case, the ionization wave originating at one nucleus is scattered from the adjacent nucleus causing subsequent interference between the original and scattered waves. This phenomenon is related to the well-known extended x-ray absorption fine structure (EXAFS) technique [5,6] used in solid-state physics to study the structure of materials. Hence, while atomic ionization is generally well-understood [7,8], more subtle effects arising from coherent electron emission distinguish molecular ionization from its atomic counterpart and consequently reveal the wavelike aspects of the ejected electrons.

In Ref. [1], Young-type interference effects were observed in the electron emission spectra arising from fast $(v/c \sim 0.3)$ collisions of highly charged Kr ions with H_2. Follow-up studies for H_2 [9–11] revealed additional properties, including the angular and collision velocity dependences, of this atomic Young-type electron interference, with experimental observations being in general agreement with theoretical calculations [12–14]. These results prompted new studies for H_2 by other investigators [15–18]. Fast electrons $(v/c \sim 0.1)$ interacting with D_2 were also found to exhibit Young-type interferences [19]. Additionally, secondary oscillatory structures superimposed on the primary interference pattern and attributed to intramolecular scattering were observed for collisions of Kr^{33+} [10] and H^+ [11] with H_2.

The primary Young-type interference structures have been found to depend strongly on the electron observation angle [9,11], with little structure for 90°, and to a lesser extent on the collision velocity [11]. In contrast, the secondary interference structures, with approximately double the oscillation frequency, showed little variation with either the emission angle or the collision velocity [10,11], and notably showed equally strong oscillatory structures at 90° as for other angles. The primary Young-type interferences and also the secondary structures have been formulated using methods of both wave optics and quantum mechanics, establishing a sound theoretical basis for the observed interferences [20]. To date, electron interferences in diatomic molecules more complicated than H_2 or D_2 have only been studied for the photoionization of particular valence electrons from N_2 and O_2 [2,3] and for the ejection of *K*-shell electrons in CO [21,22] and N_2 [23].

In the present work, interferences associated with electron ejection are investigated for N_2 impacted by 1–5-MeV H^+ ions. For diatomic molecules such as N_2 ionization can occur from several molecular orbitals, as opposed to the single *K*-shell orbital in H_2. However, the probability for ionization of the valence *L*-shell orbitals in N_2 is about three orders of magnitude larger than for the *K*-shell orbitals [7,8], which are not expected to contribute significantly to any interference effects. To reveal the relatively small expected interference structures superimposed on "backgrounds" of exponentially decreasing cross sections, the measured molecular N_2 cross sections are normalized to corresponding theoretical atomic N cross sections according to

$$(\sigma_{N_2})_{\text{norm}} = \frac{d^2\sigma_{N_2}}{d\Omega d\varepsilon} \Big/ \frac{d^2\sigma_{2N}}{d\Omega d\varepsilon}, \tag{1}$$

where $d\Omega$ is the solid angle for electron detection and $d\varepsilon$ refers to the outgoing electron energy. The cross section σ_{N_2} denotes molecular two-center emission and σ_{2N} is the cross section for independent emission from the two N atoms [1]. In Ref. [12] it was shown that for H_2 this normalized ratio of cross sections exhibits primary Young-type electron interferences with a damped oscillatory behavior approximated by the function $[1+\sin(k_\parallel - q)d]/[(k_\parallel - q)d]$, where $k_\parallel$ is the outgoing electron momentum component parallel to the beam

 ©2008 The American Physical Society

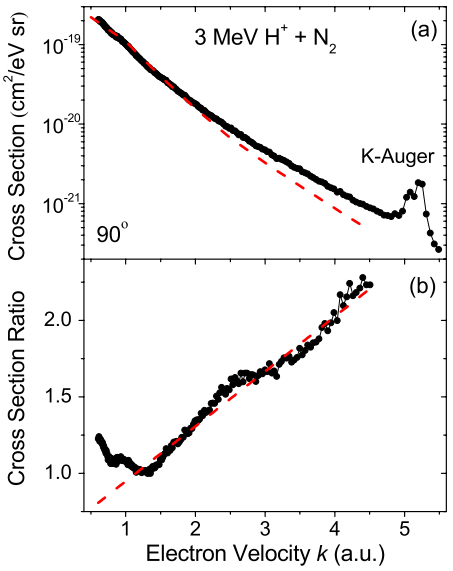

FIG. 1. (Color online) (a) Measured N_2 cross sections (solid circles) and calculated theoretical N cross sections (dashed line) for 3-MeV $H^+ + N_2$ at 90° observation angle. (b) Ratio of the measured and theoretical cross sections from (a), along with a linear fit (dashed line) to the resulting ratio (see text).

direction, i.e., $k_\parallel = k\cos\theta$ (θ is the electron observation angle), q is the minimum momentum transfer, and d is the internuclear separation. This predicted angular dependence for the Young-type interferences was verified in Refs. [9,11].

II. THEORY

The theoretical atomic N cross sections needed to normalize the experimental molecular N_2 cross sections according to Eq. (1) were calculated using a first-order impact parameter method. The initial state of the N atom has been described by a Hartree-Fock wave function, while the wave function of the ejected electron has been calculated in the field of the residual ion. The overall shapes of the calculated atomic N cross sections generally agree with the measured N_2 yields, except at higher electron energies where the theory falls off faster than the measured data as seen in Fig. 1(a) (also see Ref. [24]).

Additionally, to compare the experimentally observed oscillatory structures with the expected primary Young-type interference structures, we have performed theoretical calculations for the ionization of N_2 obtaining molecular to atomic cross section ratios. The model takes into account only the first-order interference effects caused by the two-center character of the initial wave function and is similar to the formulation developed by two of the present authors for H_2 [12]. The main difference is that N_2 has several molecular orbitals giving different interference patterns. The $1s\sigma_g$ and the $2s\sigma_g$ bonding orbitals of N_2 have the same symmetry as the occupied orbital of H_2, and the cross section may be expressed by the same formula as in our previous paper [12]

$$\frac{d\sigma}{d\Omega_k dk} = C + G\frac{\sin a}{a}. \tag{2}$$

Here $a = d(k_\parallel - q)$, where $k_\parallel$ is the parallel component of the ejected electron momentum relative to the projectile velocity and q is the minimum momentum transfer ($q = \Delta E/v_p$; ΔE is the energy transferred to the ejected electron and v_p is the projectile velocity). The interference effect for the $1s\sigma_u^*$ and the $2s\sigma_u^*$ antibonding orbitals may be treated similarly, but the interference term has the opposite sign

$$\frac{d\sigma}{d\Omega_k dk} = C - G\frac{\sin a}{a}, \tag{3}$$

and thus the effects of these two pairs of orbitals cancel each other and do not contribute to oscillations in the cross section ratio.

The calculations for the other two occupied orbitals of N_2, namely $2p\sigma_g$ and $2p\pi_u$, are different, however, because of their more complicated angular dependence. The wave functions of these orbitals are expressed in the molecular frame and then transformed using the Wigner three-dimensional (3D) functions into the laboratory frame. The integration is performed over the trajectory of the projectile similar to that done in Ref. [12]. Moreover, taking into account only the fast oscillating term in the expression for the transition probability [analogous to Eq. (16) of Ref. [12]], the average over the orientation of the molecular axis may be done analytically. Owing to the angular dependence, the final expression for the cross sections of the $2p\sigma_g$ and $2p\pi_u$ orbitals has several terms

$$\frac{d\sigma}{d\Omega_k dk} = C + G_1\frac{\sin a}{a} + G_2\frac{\sin a}{a^3} + G_3\frac{\sin a}{a^5} + G_4\frac{\cos a}{a^2} + G_5\frac{\cos a}{a^4}, \tag{4}$$

where the values of the quantities C and G_i depend on the type of the orbital and on the momentum of the ejected electron.

III. EXPERIMENT

The present measurements were conducted at Western Michigan University using the 6-MV tandem Van de Graaff accelerator. H^+ beams with energies 1, 3, and 5 MeV and intensities ~40–500 nA were collimated to a diameter of ~1.5 mm and directed into the scattering chamber onto a N_2 gas target. A collimator biased to +400 V located at the entrance of the scattering chamber was used to reduce the number of low energy electrons from slit scattering. The N_2 target was supplied by a gas jet of diameter ~1.8 mm positioned ~3.5 mm above the center of the beam line. The gas flow rate was adjusted to maintain an average pressure of ~50 times the background pressure in the scattering chamber, which was $\sim 1\times 10^{-6}$ Torr. Measurements were taken for different gas pressures to verify the existence of single collision conditions. Electrons emitted from the target gas were measured for ejection energies 5–410 eV and observation angles 30°, 45°, 60°, 90°, 120°, 135°, and 150° with respect to the incident beam direction using an electrostatic parallel-plate analyzer equipped with a channel electron multiplier. The electron spectra were normalized to the incident beam intensity. Background spectra were recorded with no

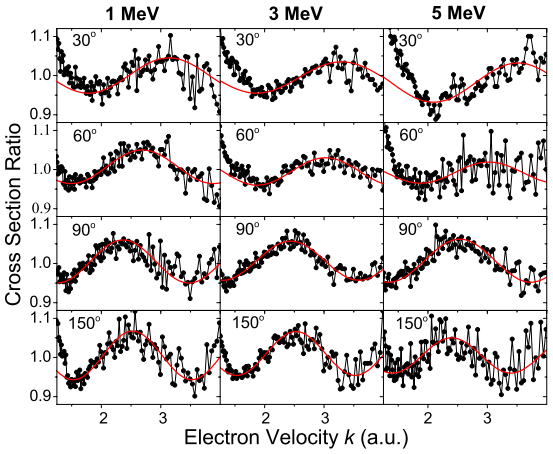

FIG. 2. (Color online) Ratios obtained by dividing the measured molecular N_2 cross sections by atomic N cross sections and subsequently by a linear function [see Fig. 1(b)] to correct for the discrepancy between experiment and theory at high electron ejection energies [see Fig. 1(a)]. Results shown are for 1, 3, and 5-MeV H^+ ions at the indicated observation angles. The smooth curves are the results of fitting Eq. (5) to the ratios.

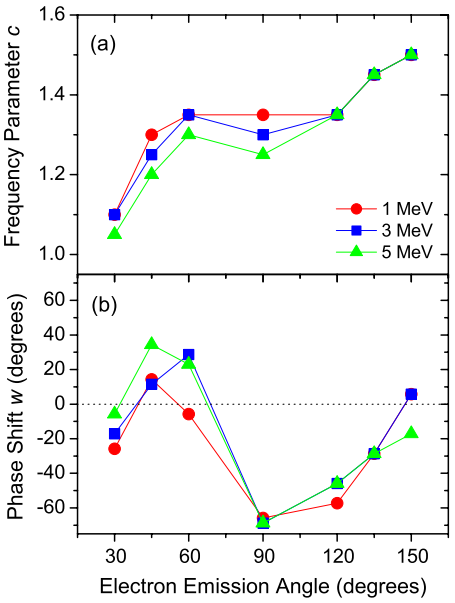

FIG. 3. (Color online) Frequency parameters c and phase shifts w obtained by fitting Eq. (5) to the data of Fig. 2 are shown for all measured angles at projectile energies of 1, 3, and 5 MeV. The uncertainties in c are about ± 0.1 and in w about $\pm 5°$.

target gas to correct for residual gas events. Shielding with a μ-metal liner minimized stray magnetic fields inside the scattering chamber.

IV. RESULTS AND DISCUSSION

The measured molecular N_2 electron emission yields, as shown in Fig. 1(a) for 90°, were divided by the corresponding theoretical atomic N cross sections, giving ratios as shown in Fig. 1(b). The ratios, normalized to about unity for convenience, show clear evidence of oscillatory behavior with a rising trend at high electron energies due to the discrepancy between the measured data and the theory seen in Fig. 1(a). A similar rising trend was observed previously for $Kr^{34+}+H_2$ collisions [1]. To eliminate the overall rising trend and to better reveal the oscillatory structures, a linear function, shown by the dashed line in Fig. 1(b), was fit to the cross section ratios as in Ref. [1]. Using this fitting procedure for all observation angles and beam energies, the cross section ratios were then divided by the linear function to give the experimental-to-theoretical ratios shown in Fig. 2.

The striking feature of the ratios shown in Fig. 2 is that the oscillatory structures show no significant dependence on the electron observation angle or the collision velocity, nor does their magnitude appear to decrease with increasing k, i.e., there is no apparent damping. Moreover, the structures for 90° are as prominent as for the other angles. These results are contrary to those for H^+ [11] and Kr^{33+} [9] $+H_2$ for which the primary Young-type interference structures showed a strong dependence on the observation angle, with no oscillatory structure for 90°, and a smaller but definite dependence on the collision velocity. As noted above, the observations for H_2 were in general agreement with theoretical predictions of the primary Young-type interference [12–14].

Thus, the observed oscillatory structures for N_2 suggest an origin other than primary Young-type interferences, and, in fact, are suggestive of the previously observed secondary interferences that have been attributed to interference of the primary ejected electron wave with the secondary wave that results from scattering at the other atomic center [10,11]. These secondary oscillations can be interpreted from phase differences in the scattering process [10,20] and differ from the primary Young-type structures in that the secondary interferences are governed simply by the electron momentum k rather than by $|\mathbf{k}-\mathbf{q}|$, with the consequence that there is negligible dependence on electron observation angle or collision velocity. Moreover, the theoretical formulation predicts a secondary oscillation frequency about double that of the primary frequency resulting from the additional phase acquired by propagation of the primary electron wave along the internuclear axis from one atomic center to the other, a result that is consistent with the model of Kronig [4].

To quantitatively characterize the oscillatory structures and frequencies for N_2, the normalized cross section ratios of Fig. 2 were parametrized according to the function

$$f(k) = A[1 + \sin(kcd - w)] + B, \tag{5}$$

where, in addition to the previous definitions for k and d, c is a fitting parameter representing the oscillation frequency, w allows for a phase shift, and A and B are normalization constants. Allowance for a phase shift was also utilized in Refs. [10,11] to describe the secondary interference structures attributed to intramolecular scattering. This equation is similar to Eq. (2), except that there is no damping, nor does the minimum momentum transfer (q) appear.

The values obtained for c and w from the fitting are shown in Figs. 3(a) and 3(b), respectively. The frequency parameter c [Fig. 3(a)] shows only a small dependence on the electron observation angle (note the suppressed ordinate)

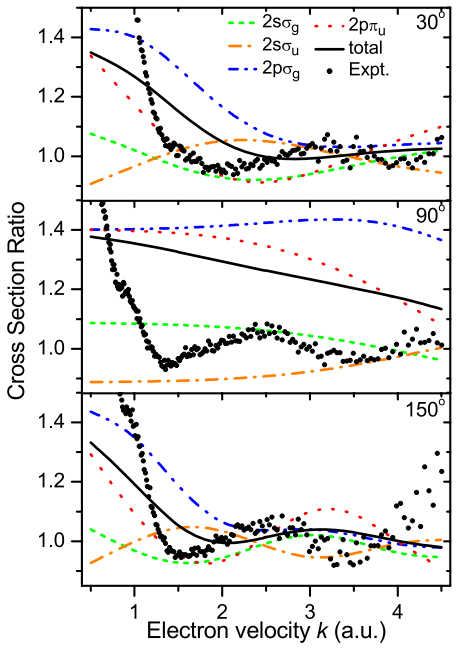

FIG. 4. (Color online) Theoretical first-order ionization cross-section ratios for 3-MeV H^+ impact on N_2 for electron observation angles of 30°, 90°, and 150° as a function of ejected electron velocity in comparison to the experimental data. The contributions for the individual molecular orbitals of N_2, i.e., $2s\sigma_g$, $2s\sigma_u^*$, $2p\sigma_g$, and $2p\pi_u$ were calculated according to Eqs. (2)–(4) (see text).

and the collision velocity in sharp contrast to results for the primary interferences in H_2 [9,11,25]. By way of comparison, the first-order Young-type interferences observed for $Kr^{33+}+H_2$ and $H^+ + H_2$ collisions gave values for c that exhibited approximately a cos θ dependence, with a value close to zero for observation angles near 90° [9,11,25]. On the other hand, the second-order oscillations for these same collisions gave values for c in the range ~2.5–3 that were nearly independent of the observation angle. Regarding the phase shift w, Fig. 3(b) shows this parameter to have a maximum around 45° and a minimum at 90°, with little dependence on the collision velocity. The presence of this shift can be seen already by careful examination of the cross section ratios in Fig. 2. On the contrary, the second-order oscillations in $Kr^{33+}+H_2$ and $H^+ + H_2$ exhibited a constant phase shift of $w \sim \pi$ [10,11]. The exact reason for the angular dependence of this phase shift is presently unknown, but is likely contained in the amplitude factors governing the secondary interferences (see Refs. [10,20]).

To provide further insight into the present results, we have performed theoretical calculations for the ionization of N_2 to derive the expected oscillatory behavior of the molecular-to-atomic cross section ratios for the first-order Young-type interferences as discussed above in Sec. II. The results of these first-order calculations for the cross section ratios are presented in Fig. 4 along with the experimental data. It is clear from the calculations for the individual molecular orbitals, in particular the contributions due to $2s\sigma_g$ and $2s\sigma_u^*$ as given by Eqs. (2) and (3), respectively, that the different symmetries of these orbitals cause a significant part of the first-order oscillations in the total cross section ratios to cancel and, consequently, these structures are suppressed. A similar cancellation occurs for the $1s\sigma_g$ and $1s\sigma_u^*$ orbitals (not shown in Fig. 4). On the other hand, the contributions from $2p\sigma_g$ and $2p\pi_u$ as given by Eq. (4) do not cancel and are responsible for essentially all of the expected first-order (Young-type) interference structure for N_2.

The resulting predicted structure for each angle is a decreasing (damped) ratio for increasing electron velocity with some oscillations remaining, most prominently at 150°. As may be observed from Fig. 4, the experimental data oscillate around the first-order theoretical results; however, it is difficult to unambiguously identify any primary Young-type oscillations, a result that is in sharp contrast to previous studies for H_2 targets [1,9,11]. This comparison between the measured and predicted ratios indicates that the experimentally observed oscillations for N_2 shown in Fig. 2 do not originate from the primary Young-type interferences. Instead, we attribute these higher frequency oscillations to secondary interferences arising from intramolecular scattering, as previously observed for electron emission from H_2 [10,11]. To the extent that this conclusion is valid, the present results for 1–5-MeV $H^+ + N_2$ collisions indicate that the observed oscillatory structures are due mainly to secondary interferences while the primary interferences are strongly suppressed. We note, however, that the first-order theoretical calculations indicate that some structure from primary oscillations should be observed.

If the observed oscillatory structures in Fig. 2 are indeed due to secondary interferences, then the underlying mechanism for their production must be understood. Previously, we conjectured that these secondary structures originated from ejection of a K-shell electron at one atomic center followed by scattering at the adjacent nucleus [24], reasoning that these core electrons are highly localized and hence cannot undergo coherent emission from both centers. However, because ionization of a K-shell electron is about three orders of magnitude smaller than for a valence (L-shell) electron, it is not likely that core ionization is the origin of the observed structures. On the other hand, it might be argued that secondary interference occurs when an L-shell electron undergoes large momentum transfer in a relatively "hard" binary encounter, causing the electron to scatter off the adjacent nucleus, leading to interference between the initial L-shell ionizing event and the subsequent secondary scattering event. Such scattering is similar to that resulting from the core ionization of heteronuclear molecules discussed by Kronig [4], and also to that observed in EXAFS studies [5,6], for which oscillations occur in the energy region just above the threshold for core ionization. Notably, in both cases the oscillatory part of the spectra are described by a function of the form $\sin(2kd+\delta)$ (δ is a phase shift), which is remarkably similar to Eq. (5). The reason that c in Eq. (5) does not give the value two may be due to the fact that ionization of N_2 by fast ions involves mainly valence electrons, which can occur from several orbitals. However, theoretical calculations to verify such an explanation for the present case of $H^+ + N_2$ collisions are beyond the scope of the present work and further theoretical and experimental investigations are needed.

The present results can also be compared to those for photoionization of N_2. In the case of K-shell photoionization

[23], the localized nature of the *K* electrons suppresses Young-type interferences because the ejected electron is not coherently emitted from both centers. On the other hand, ionization of the valence electrons produces modulations in the resulting cross sections that have been attributed to Young-type interference [2,3]. The principal difference between photoionization of N_2 and ionization by fast ion impact is, of course, the fact that in the former case the photon energy can be chosen to selectively remove electrons from a particular orbital. Such selective ionization does not occur for fast ions, although, as noted above, the present work for 1–5-MeV/u H^+ impact is not expected to lead to significant *K*-shell ionization [7,8]. Moreover, the fact that there are several *L* orbitals delocalized over the molecule might be the reason that primary Young-type interferences are strongly suppressed for ionization of N_2 by fast ions. Indeed, the theoretical calculations shown in Fig. 4 suggest such a suppression.

V. CONCLUSION

In summary, there seem to be fundamental differences between H_2 and N_2 targets in giving rise to interferences in electron emission. In particular, for N_2 primary interferences are apparently suppressed, while secondary structures characterized by their independence on observation angle and collision velocity are clearly visible. Based on comparison with observations for H_2 these secondary structures are attributed to interferences resulting from intramolecular scattering. It is suggested that these secondary interferences originate in a binary encounter of the projectile with a valence electron leading to subsequent scattering at the adjacent atomic center. Quantitative calculations predicting the frequency and magnitude of these secondary oscillations, which remain a significant challenge for theory, are needed to unambiguously determine if the observed structures indeed have their origin in intramolecular scattering. Additionally, similar measurements for other diatomic molecules such as O_2 may shed light on these structures. The differences in the oscillatory structures observed for H_2 and heavier molecules such as N_2 further highlight the unique character of molecular ionization compared to atomic ionization.

ACKNOWLEDGMENTS

The authors acknowledge helpful discussions with Dr. N. Stolterfoht regarding the interpretation of the results. Three of the authors (F.J-S., K.P., and L.N.) were supported by the Romanian National Plan for Research (PN II) under Contract No. ID-539.

[1] N. Stolterfoht *et al.*, Phys. Rev. Lett. **87**, 023201 (2001).
[2] J. A. R. Samson and R. B. Cairns, J. Opt. Soc. Am. **55**, 1035 (1965).
[3] H. D. Cohen and U. Fano, Phys. Rev. **150**, 30 (1966).
[4] R. de L. Kronig, Z. Phys. **75**, 468 (1932); H. S. W. Massey and E. H. S. Burhop, *Electronic and Ionic Phenomena* (Clarendon Press, Oxford, England, 1952), p. 201.
[5] B. K. Teo, *EXAFS: Basic Principles and Data Analysis* (Springer, Berlin, 1986).
[6] D. C. Koningsberger and R. Prins, *X-Ray Absorption, Principles, Techniques of EXAFS, SEXAFS and XANES* (Wiley, New York, 1988).
[7] M. E. Rudd, Y. K. Kim, D. H. Madison, and T. J. Gay, Rev. Mod. Phys. **64**, 441 (1992).
[8] N. Stolterfoht, R. D. Dubois, and R. D. Rivarola, *Electron Emission in Heavy Ion-Atom Collisions*, Springer Series on Atoms and Plasmas (Springer, Heidelberg, 1997).
[9] N. Stolterfoht *et al.*, Phys. Rev. A **67**, 030702(R) (2003).
[10] N. Stolterfoht, B. Sulik, B. Skogvall, J. Y. Chesnel, F. Fremont, D. Hennecart, A. Cassimi, L. Adoui, S. Hossain, and J. A. Tanis, Phys. Rev. A **69**, 012701 (2004).
[11] S. Hossain, A. L. Landers, N. Stolterfoht, and J. A. Tanis, Phys. Rev. A **72**, 010701(R) (2005).
[12] L. Nagy, L. Kocbach, K. Póra, and J. P. Hansen, J. Phys. B **35**, L453 (2002).
[13] M. E. Galassi, R. D. Rivarola, P. D. Fainstein, and N. Stolterfoht, Phys. Rev. A **66**, 052705 (2002); M. E. Galassi, R. D. Rivarola, and P. D. Fainstein, *ibid.* **70**, 032721 (2004).
[14] L. Sarkadi, J. Phys. B **36**, 2153 (2003).
[15] D. Misra, U. Kadhane, Y. P. Singh, L. C. Tribedi, P. D. Fainstein, and P. Richard, Phys. Rev. Lett. **92**, 153201 (2004).
[16] C. Dimopoulou *et al.*, Phys. Rev. Lett. **93**, 123203 (2004).
[17] K. Støchkel *et al.*, Phys. Rev. A **72**, 050703(R) (2005).
[18] D. S. Milne-Brownlie, M. Foster, J. Gao, B. Lohmann, and D. H. Madison, Phys. Rev. Lett. **96**, 233201 (2006).
[19] O. Kamalou, J. Y. Chesnel, D. Martina, F. Fremont, J. Hanssen, C. R. Stia, O. A. Fojon, and R. D. Rivarola, Phys. Rev. A **71**, 010702(R) (2005).
[20] N. Stolterfoht and B. Sulik, in *Advances in Quantum Chemistry*, edited by R. Cabrera-Trujillo and J. Sabin (Elsevier Science, New York/Academic Press, New York, 2004), Vol. 46, pp. 307–327.
[21] F. Heiser, O. Gessner, J. Viefhaus, K. Wieliczek, R. Hentges, and U. Becker, Phys. Rev. Lett. **79**, 2435 (1997).
[22] A. Landers *et al.*, Phys. Rev. Lett. **87**, 013002 (2001).
[23] D. Rolles *et al.*, Nature (London) **437**, 711 (2005).
[24] J. L. Baran, S. Das, F. Járai-Szabó, L. Nagy, and J. A. Tanis, J. Phys.: Conf. Ser. **58**, 215 (2007).
[25] J. A. Tanis, J. Y. Chesnel, B. Sulik, B. Skogvall, P. Sobocinski, A. Cassimi, J. P. Grandin, L. Adoui, D. Hennecart, and N. Stolterfoht, Phys. Rev. A **74**, 022707 (2006).